Using Granger Causality to assess the interaction between brain areas during different consciousness states

Rita Pizzi, Teresa Rutigliano, Marialessia Musumeci and Massimo Pregnolato

Abstract**—**To analyze cortico-cortical interactions in different consciousness states, namely during NREM sleep and wakefulness, we compared evoked potentials from 5 mA intra-cerebral stimulations in an epileptic subject undergoing clinical evaluation. We collected recordings from 16 different cortical areas and analyzed the perturbation effects in a 200ms time range after the stimulus using both cross-Coherence and Granger causality and comparing the two procedures. Results show that the overall interaction intensity involves a wider frequency range during wakefulness than during NREM sleep. Moreover, comparing similar Coherence intensity thresholds, the number of interacting areas is sharply higher during wakefulness. However, during the NREM phase, interactions show a highly directional behavior that is not present during wakefulness. The study displays which areas are mainly involved in reciprocal G-causal interactions, paving the way to a following research on their functional meaning.

Keywords**—**Autoregressive model, Granger Causality, Coherence, Consciousness, NREM Sleep, SEEG.

I. Introduction

THE generalized goal in computational neuroscience is to create a model able to describe the brain dynamics, at different possible levels of spatial resolution [1][2] , where levels are categorized as micro-scale, mesoscale and macro-scale. Electrophysiological and neuroimaging techniques refer to the macro-scale brain dynamics.

With the purpose to improve our knowledge on brain dynamics at a macro-scale we analyzed data obtained from multi-contact intracerebral electrodes placed deep in the human cortex. In particular, we aimed to explore the dynamical evolution of a neural network when an intracranial electrical perturbation occurs. We used connectivity measures based on the mathematical properties of the underlying linear autoregressive process (AR) in order to estimate spectral quantities, in particular spectral Coherence and Granger Causality, analyzed with bivariate models. We focused on spectral Coherence as a measure of the amount of interdependency between channels and on Granger Causality [3][4][5][6] implemented according to Geweke's formulation [7] in order to get the direction of the causal influence.

This work was supported by the Department of Computer Science, University of Milan, Via Bramante 65, 26013 Crema CR, Italy.

R. Pizzi is Senior Researcher at the Department of Computer Science, University of Milan, Via Bramante 65, 26013 Crema CR, Italy (corresponding author; phone: +39 02 503 30072; fax: 02 503 30010; e-mail: rita.pizzi@unimi.it).

T. Rutigliano is PhD Student at the Department of Computer Science, University of Milan, Via Bramante 65, 26013 Crema CR, Italy (e-mail: teresa.rutigliano@unimi.it).

M. Musumeci is PhD Student at the Department of Computer Science, University of Milan, Via Bramante 65, 26013 Crema CR, Italy (e-mail: marialessia.musumeci@unimi.it).

M.Pregnolato is Associate Professor at the Department of Pharmaceutical Chemistry, University of Pavia, Viale Taramelli 12, 27100 Pavia , Italy (e-mail: massimo.pregnolato@unipv.it).

II. Materials and Methods

Electrophysiological data were acquired by intracerebral recordings. A subject with drug-resistant focal epilepsy participated in the study [8], [9] ; during pre-surgical evaluation SEEG (stereo-EEG) platinum–iridium semi-flexible electrodes (Dixi Medical [10] : diameter 0.8 mm, contact length 1.5 mm, inter-contact distance of 2 mm, up to 18 contacts per electrode) were implanted in order to record signals during a single pulse electrical stimulation session.

The patient gave written informed consent before intracerebral multi-lead electrode implantation and the procedure was approved by the Local Ethical Committee [8].

The stimulation session was applied at a single channel, here indicated as S3 (superior central) and SEEG recordings were obtained from all other 147 channels. A single stimulation session consists of 30 impulses at intervals of 1 s, each impulse is 0.2 ms long, stimulation of strength 5mA [9].

In our analysis we considered a subset of 16 bipolar recordings selected in absence of epileptic seizure, positioned in grey matter [8], selected on the basis of their distance from the stimulation site (S3). The list of channels involved in the process is reported in Fig.1C. For this work we used two datasets where the difference is the timing of recording data: namely a dataset has only data collected during the waking state of the patient (from now on WAKE) and the other presents data collected during the state of N3 sleep stage (from now on SLEEP). Each available dataset has 3000 samples at a sampling frequency equal to 100 Hz, corresponding therefore to 30 seconds.

Knowing that the electrical pulse lasts 0.2 ms and is repeated every 1 second, we can confirm that our dataset contains 30 pulses. The first 200 milliseconds of each second include the stimulation trigger. Our intent is to analyze this

period immediately following the stimulus, including the stimulus itself because its short duration makes it irrelevant in the analysis.

Data were collected during wakefulness and we analyzed a time window of 30 seconds at 100Hz sampling frequency. Data were pre-processed with band-pass filtering (0.5-300Hz) using a third order Butterworth filter and calculating ensemble mean divided by standard deviation. Artefacts were reduced with a Tukey[8] [9] windowed median filtering. In Fig.1 electrode positions are shown: in the A panel electrodes localization using Econnectome, a Matlab toolbox [11] [12] [13]; in the B panel a 3-dimensional localization using Matlab commands; in the C panel the list of channels and their anatomical localization.

In order to process signals we used Matlab with the following plugins: EEGLAB [14], Bsmart [6], Econnectome [11]. In Bsmart we built Bivariate Autoregressive models in order to obtain the parameters needed to compute the aimed Coherence and Causality networks. While Coherence spectra do not show the direction of the information flow among channels [7] [15], Granger Causality theory provides a tool to identify oriented interactions from time-series data. Granger [3] defined causal influence in terms of stochastic processes: one stochastic process is causal to a second if the autoregressive predictability of the second process at a given time point is improved by including measurements from the immediate past of the first. Then a variable A will Granger-cause B if B can be predicted using the past of A and B so that we can determine an "information flow" from A to B .

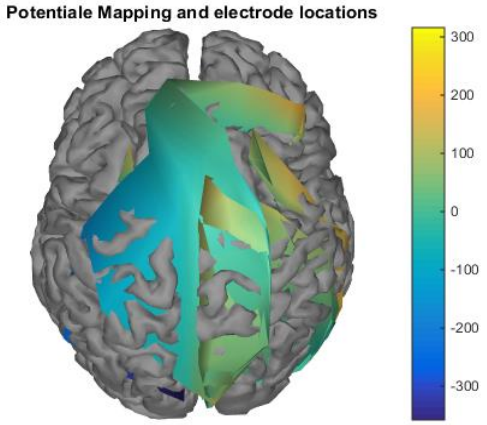

(a)

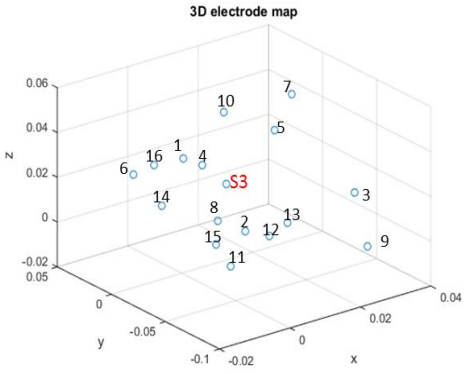

(b)

Channel	Anatomical position
1	'G_precentral'
2	'S_interm_prim-Jensen'
3	'G_pariet_inf-Angular'
4	'Medial_wall'
5	'S_temporal_sup'
6	'G_front_middle'
7	'G_and_S_cingul-Mid-Ant'
8	'S_intrapariet_and_P_trans'
9	'S_oc_sup_and_transversal'
10	'S_front_sup'
11	'S_temporal_sup'
12	'S_intrapariet_and_P_trans'
13	'S_parieto_occipital'
14	'G_and_S_cingul-Mid-Post'
15	'S_temporal_sup'
16	'G_temporal_middle'

(c)

Fig. 1 Electrode localizations: (a) Potentials map. (b) 3-dimensional electrode map. (c) List of channels and their anatomical localization (Destrieux Atlas) [16].

We can say that Granger Causality is a concept homologous to the transfer entropy, a direct version of Shannon's mutual information [17] [18].

After obtaining the bivariate autoregressive model for two time series x_{1t} and x_{2t}, according to Geweke's formulation [7] the Granger causal influence from x_{2t} to x_{1t} is given by (1):

$$I_{2\to 1}(f) = -\ln\left(1 - \frac{V_{22} - \frac{V_{12}^2}{V_{11}}\left|H_{12}(f)\right|^2}{S_{11}(f)}\right) \qquad (1)$$

where V_{11}, V_{22}, V_{12} are elements of the noise covariance matrix, H_{12} is element of the transfer function derived by the model's coefficients matrix, and S_{11} is the power spectrum of channel 1 at frequency f [5] .

The time-domain Granger Causality from x_{2t} to x_{1t} can be interpreted as the reduction in the unexplained variance of x_{1t}, as computed solely from the past values of x_{1t}, that comes from subsequent inclusion of past values of x_{2t}. The size of this reduction can be viewed as the ''amount of variance'' of x_{1t} explained by the history of x_{2t} .

The variance ratio is obtained from the Granger Causality value at a given frequency as $1 - e^{-I(f)}$, where *I(f)* denotes the Granger Causality value at frequency *f*.

III. Results

In order to process the AR model, we set the Akaike Information Criterion (AIC) to determine the model order, evaluating 3 as the optimal choice (Fig. 2) both for the WAKE and for the SLEEP data sets.

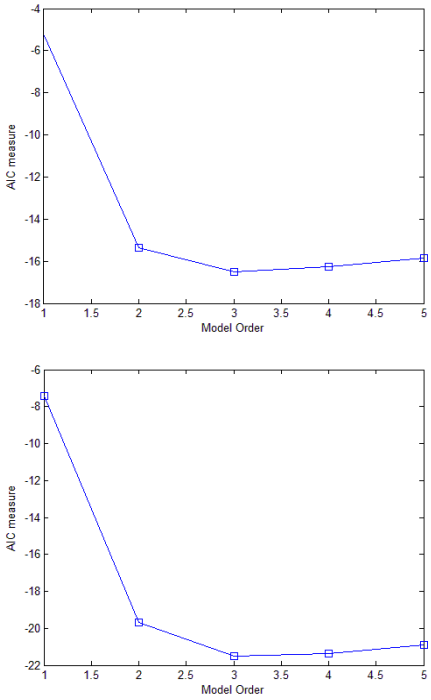

Fig. 2 AIC graphs for model order determination: WAKE (above) and SLEEP (below).

Once created both the bivariate moving window models with order 3, we tested them with whiteness and stability tests. As the residuals autocorrelation results to be close to zero, this means that the residual noise is white and the model represents correctly the autoregressive process. The stability index maintains itself nearly always below zero, further validating the models.

We evaluates the spectral Coherence [4] and the Granger Causality of the autoregressive models analyzing both the WAKE (Fig. 3a, 3b) and the SLEEP (Fig. 4a, 4b) signals. Below we present the results of our investigation.

In WAKE:

The Coherence network shows the following connections:

1-14, 1-4, 1-13, 1-6, 1-7, 2-14, 4-14, 4-10, 4-13, 6-14, 7-14, 10-13, 10-14, 13-14.

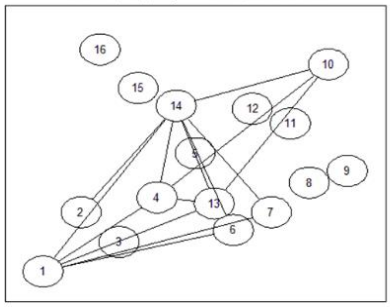

Fig. 3a Coherence network

The Granger Causality network shows the following oriented connections:

1>2, 1>10, 2>6, 4>13, 7>10, 10>1, 10>13, 12>10, 12>7, 12>16,13>7, 14>13,>14>2.

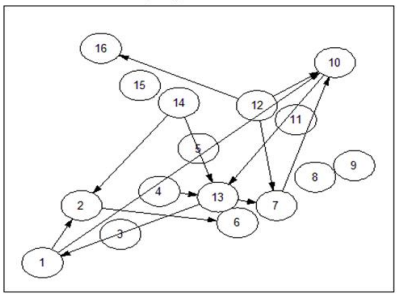

Fig. 3b G-Causality network

In SLEEP:

The Coherence bivariate analysis shows the following connections:

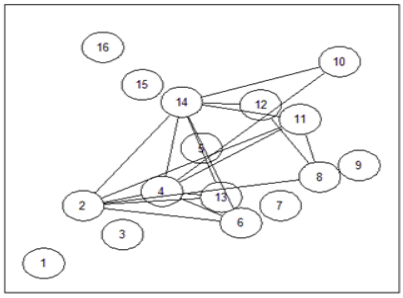

Fig. 4a Coherence network

2-14, 2-11, 2-4, 2-8, 2-13, 2-6, 4-11, 4-14, 4-10, 4-13, 4-6, 6-14, 8-11, 8-12, 10-14, 11-14,12-14,13-14.

The Granger Causality analysis shows the following oriented connections:

1>14, 1>11, 1>13, 1>8, 2>6, 6>14, 6>4, 8>14, 14>12, 15>4

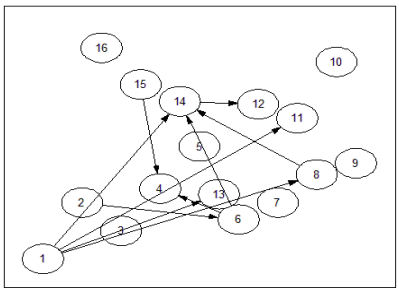

Fig. 4b G-Causality network

Then we applied a criterion to select a smaller and more significant number of connections.

Coherence and Granger Causality are two different non-overlapping procedures. It is well known that correlation and causation are very different concepts (the first does not imply the second) and since the spectral coherency is the Fourier transform of the cross-correlation(therefore the frequency-domain representation of the cross-correlation), regarding the inference or causation of the information flow, the same limitations of cross-correlation hold for coherency and its magnitude-squared counterpart, the Coherence.

However, as a G-causal connection that does not show high cross-Coherence lacks another important element of interest, we used the criterion to select the G-causal connections that show simultaneously also high spectral Coherence.

Thus the intersection between the pairs of channels identified in this way are:

WAKE:

4>13, 10>13, 14>2, 14>13

SLEEP:

2>6, 6>4, 6>14, 14>12.

The above cases have been summarized in the following Tables 1,2,3,4 (WAKE) and 5,6,7,8 (SLEEP).

Table 1 WAKE 4 >13

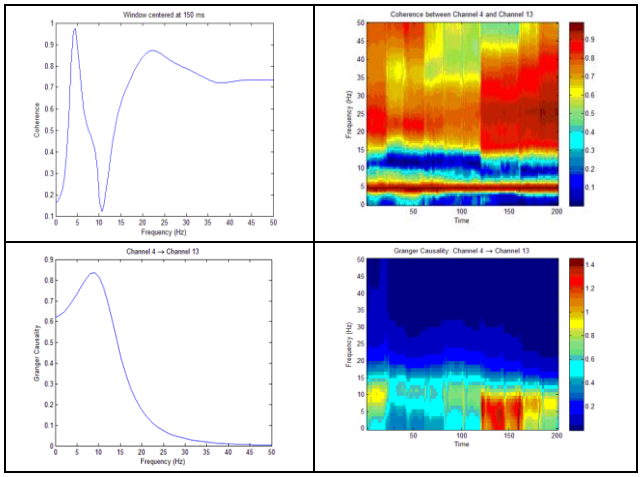

Table 2 WAKE 10>13

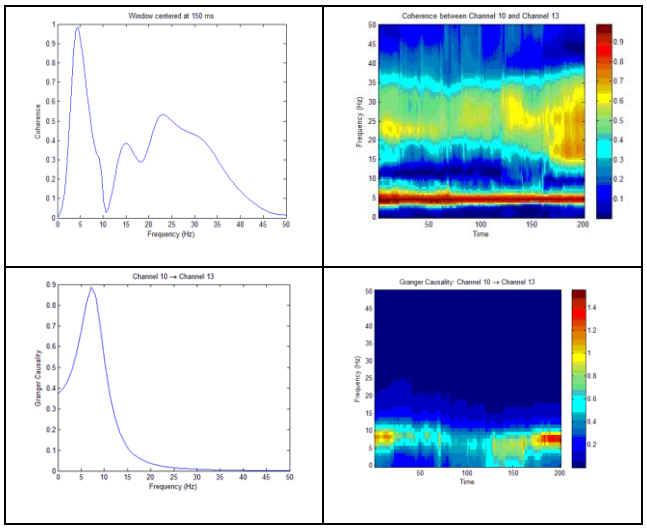

Table 3 WAKE 14>13

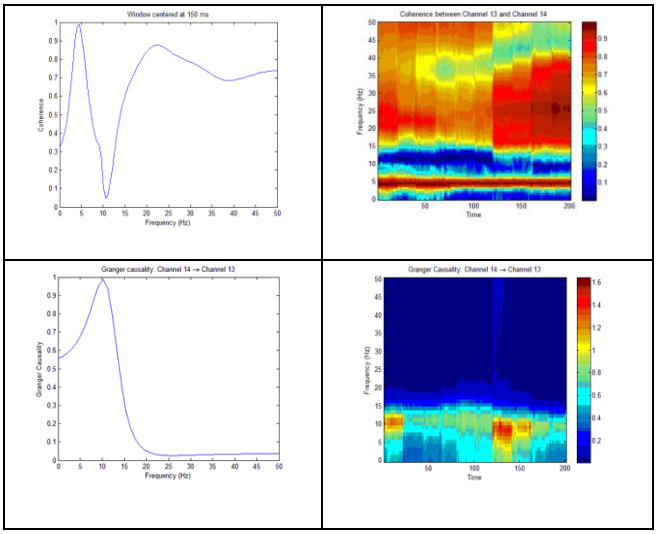

Table 4 WAKE 14>2

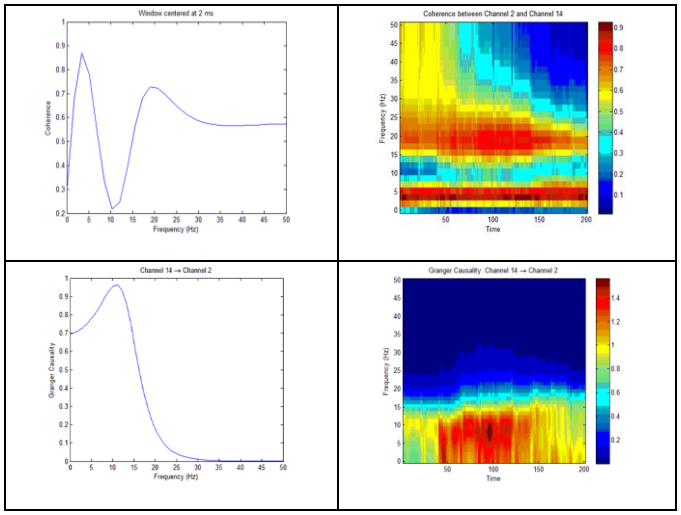

Table 5 SLEEP 2>6

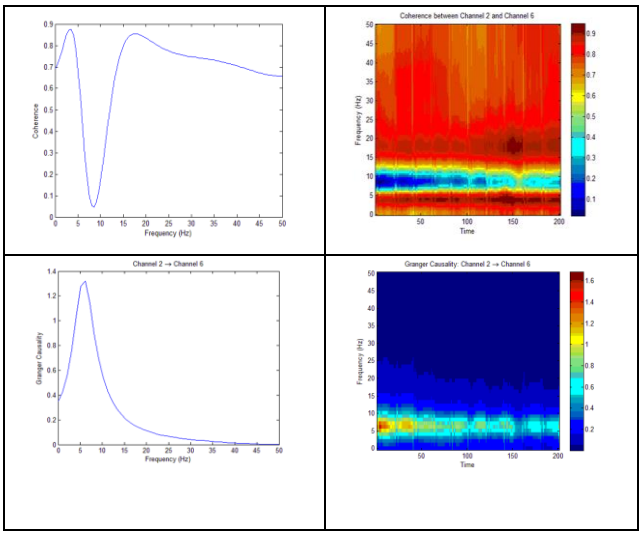

Table 6 SLEEP 6>14

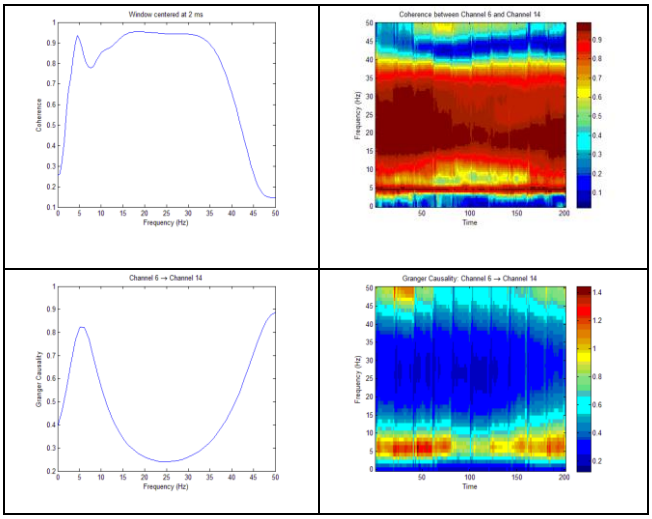

Table 7 SLEEP 14>12

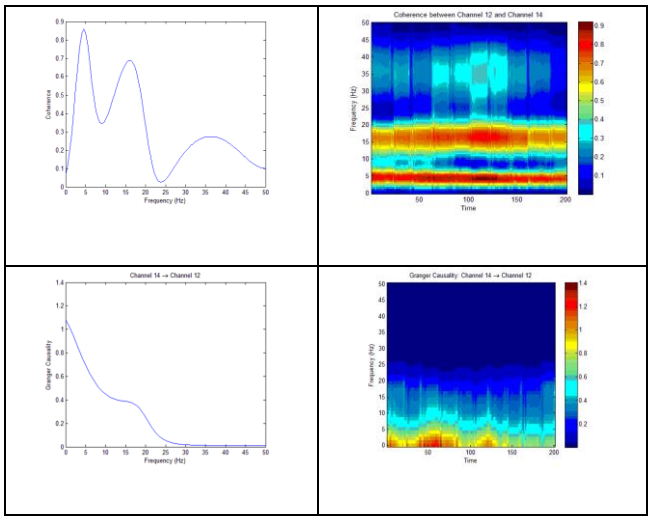

Table 8 SLEEP 6>4

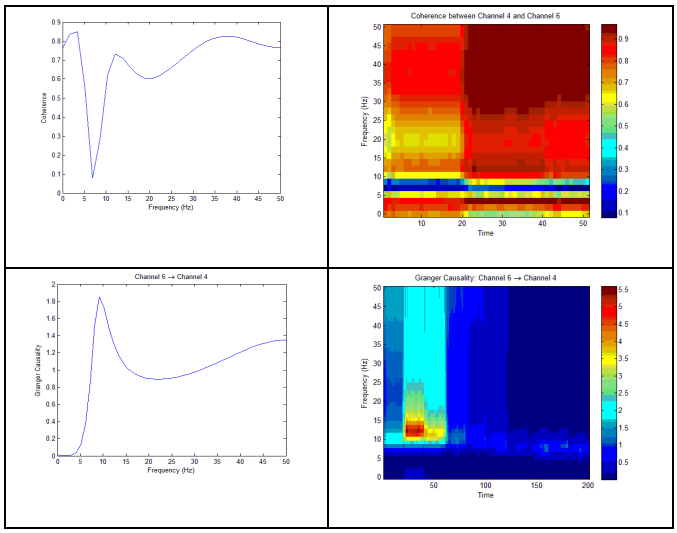

Comparing the intensity of Coherence of the signals SLEEP and WAKE at the same threshold, we can say that the number of connections is slightly greater for SLEEP (18) with respect to WAKE (14). We can also say that, in contrast to the Coherence analysis, at the same threshold, the number of connections that emerge from Granger Causality analysis is greater in WAKE (13) respect to SLEEP (10).

There are no channels with common connections between SLEEP and WAKE, but the area 14 is interesting because it is involved in both states, even if it results as a source for WAKE and a target for SLEEP.

Also interesting are the area 13, target for G-causal connections WAKE, and the area 6, source for some effects in the SLEEP signal. Interestingly, both areas, when involved, have very high levels of Coherence for a broad band of frequencies.

From the anatomical-functional point of view the most interesting areas result to be:

3: parieto-inferior angular gyrus

6: medial frontal gyrus

13: parieto-occipital sulcus

14: middle posterior part of the cingulate gyrus and sulcus.

From the spectral point of view, both SLEEP and WAKE Granger Causality and Coherence are high on the low frequencies, while the Coherence always shows a second peak at frequencies around 20Hz.

G-causality shows the highest values at very low frequencies in SLEEP (≤ 5Hz), while in WAKE it shows highest values at slightly higher frequencies (10-15Hz).

By examining the values distribution of Coherence and G-causality over time, in WAKE Coherence keeps substantially constant, while G-causality is constant only on frequencies above 10 Hz, whereas below these frequencies it tends to the maximum intensity after 100ms.

In SLEEP spectral Coherence is constant over time, while G-causality tends to opposite behavior compared to WAKE, showing, only at low frequencies, maximum values close to the stimulus (within 100ms).

In both datasets, at low frequencies G-causality often performs a refractory period of 50-100 ms after the initial reaction, followed by a reactive phase.

IV. Conclusion

The analyses performed on the recorded signals show that the considered cortico-cortical networks behave differently in NREM sleep and in wakefulness. In particular, it has not been shown any decline of connectivity during the NREM phase, which could be connected to a lower level of consciousness.

In addition, there was no evidence of common connections between areas in both states, even if area 14 seems to be affected by intense connections during both WAKE and SLEEP.

In general, the connectivity appears to be higher at low frequencies (<10 Hz).

Furthermore, it is observed that responses to the electrical stimulation result to vary over time and frequencies, in particular as regards the G-causal connections, where the response becomes evident at frequencies below 10 Hz and is diversified over time. In particular, during NREM sleep the response appears earlier and steadier.

The meaning of the described relationships between WAKE and SLEEP Coherence and G-causality networks will be investigated in the future, in order to find a possible functional meaning.

To confirm the above considerations and to yield a complete set of results useful for a better functional

understanding of the highlighted cortico-cortical connections, it will also be needed to compare the presented analyses with the analyses of signals from other patients recorded during the same experimental study.

ACKNOWLEDGMENT

We thank Prof. M. Massimini and Ing. A. Pigorini (Department of Biomedical and Clinical Sciences "L. Sacco", Università degli Studi di Milano) for yielding us the signal data set and for their invaluable support.

REFERENCES

[1] R. Kötter, "Anatomical concepts of brain connectivity, " in: *Handbook of Brain Connectivity*, Jirsa VK, McIntosh AR, Eds., Berlin*:* Springer, 2007, pp. 149–167.

[2] M. Rubinov and O. Sporns, "Complex network measures of brain connectivity: Uses and interpretations," *Neuroimage*, vol. 52, no. 3, 2010, pp. 1059–1069.

[3] T. E. Society and C. W. J. Granger, "Investigating Causal Relations by Econometric Models and Cross-spectral Methods," *Econometrica*, vol. 37, no. 3, 1969, pp. 424–438.

[4] J. Toppi, M. Petti, G. Vecchiato, F. Cincotti, S. Salinari, D. Mattia, F. Babiloni, and L. Astolfi, "The effect of normalization of Partial Directed Coherence on the statistical assessment of connectivity patterns: A simulation study," in *Proc. Annu. Int. Conf. IEEE Eng. Med. Biol. Soc. EMBS*, 2013, pp. 4346–4349.

[5] J. Cui, L. Xu, S. L. Bressler, M. Ding, and H. Liang, "BSMART: A Matlab/C toolbox for analysis of multichannel neural time series," *Neural Networks*, vol. 21, 2008, pp. 1094–1104.

[6] A. K. Seth, "Causal connectivity of evolved neural networks during behavior.," *Network*, vol. 16, no. 1, 2005, pp. 35–54.

[7] J. Geweke, "Measurement of Linear Dependence and Feedback between Multiple Time Series," *J. Am. Stat. Assoc.*, vol. 77, no. 378, 1982, pp. 304–313.

[8] A. Pigorini, S. Sarasso, P. Proserpio, C. Szymanski, G. Arnulfo, S. Casarotto, M. Fecchio, M. Rosanova, M. Mariotti, G. Lo Russo, M. J. Palva, L. Nobili, and M. Massimini, "Bistability breaks-off deterministic responses to intracortical stimulation during non-REM sleep," *Neuroimage*, vol. 112, 2015, pp. 105–113.

[9] J.-Y. Chang, A. Pigorini, M. Massimini, G. Tononi, L. Nobili, and B. D. Van Veen, "Multivariate autoregressive models with exogenous inputs for intracerebral responses to direct electrical stimulation of the human brain.," *Front. Hum. Neurosci.*, vol. 6, 2012., p. 317.

[10] Dixi Medical [Online]. Available: http://www.diximedical.net/GB/?cat=24.

[11] B. He, Y. Dai, L. Astolfi, F. Babiloni, H. Yuan, and L. Yang, "eConnectome: A MATLAB toolbox for mapping and imaging of brain functional connectivity," *J Neurosci Methods*, vol. 195, no. 2, 2011, pp. 261–269.

[12] F. Babiloni, C. Babiloni, F. Carducci, P. M. Rossini, A. Basilisco, L. Astolfi, F. Cincotti, L. Ding, Y. Ni, J. Cheng, K. Christine, J. Sweeney, and B. He, "Estimation of the cortical connectivity during a finger-tapping movement with multimodal integration of EEG and fMRI recordings," *International Congress Series*, vol. 1270, 2004, pp. 126–129.

[13] C. Wilke, W. Van Drongelen, M. Kohrman, and B. He, "Neocortical seizure foci localization by means of a directed transfer function method," *Epilepsia*, vol. 51, no. 4, 2010, pp. 564–572.

[14] A. Delorme and S. Makeig, "EEGLAB: An open source toolbox for analysis of single-trial EEG dynamics including independent component analysis," *J. Neurosci. Methods*, vol. 134, vo. 1, 2004, pp. 9–21.

[15] A. Brovelli, M. Ding, A. Ledberg, Y. Chen, R. Nakamura, and S. L. Bressler, "Beta oscillations in a large-scale sensorimotor cortical network: directional influences revealed by Granger causality," *Proc. Natl. Acad. Sci. U. S. A.*, vol. 101, no. 26, 2004, pp. 9849–9854.

[16] C. Destrieux, B. Fischl, A. Dale, and E. Halgren, "Automatic parcellation of human cortical gyri and sulci using standard anatomical nomenclature," *Neuroimage*, vol. 53, no. 1, 2010, pp. 1–15.

[17] A. K. Seth, A. B. Barrett, and L. Barnett, "Granger Causality Analysis in Neuroscience and Neuroimaging," *J. Neurosci.*, vol. 35, no. 8, 2015, pp. 3293–3297.

[18] L. Barnett, A. B. Barrett, and A. K. Seth, "Granger causality and transfer entropy Are equivalent for gaussian variables," *Phys. Rev. Lett.*, vol. 103, no. 23, 2009.